

# Design and Control of a Supercapacitor Storage System for Traction Applications

W. Lhomme<sup>1</sup>, P. Delarue<sup>1</sup>, P. Barrade<sup>2</sup>, *Member, IEEE*,  
A. Bouscayrol<sup>1</sup>, *Member, IEEE*, A. Rufer<sup>2</sup>, *Senior Member, IEEE*

<sup>1</sup>L2EP Lille, USTL, 59 655 Villeneuve d'Ascq, France

<sup>2</sup>LEI, École Polytechnique Fédérale de Lausanne, Switzerland,

e-mail: [Walter.Lhomme@ed.univ-lille1.fr](mailto:Walter.Lhomme@ed.univ-lille1.fr), URL: <http://www.univ-lille1.fr/l2ep/>

**Abstract**— The storage system in this paper is made of supercapacitors. The main goal is to ensure an efficient energy management in a series hybrid vehicle, even if braking resistors are still needed. Design considerations are discussed. In particular the influence of the inductor resistance on the system stability is described. A Maximum Control Structure is then deduced from the Energetic Macroscopic Representation of the storage system. Comparisons between experimentation and simulation are presented in order to highlight the influence of the inductor resistor. Experiments are then carried out on a normal operating cycle.

**Keywords** – Supercapacitor; Modelling; Control System; HEV.

## I. INTRODUCTION

Nowadays, supercapacitors offer an alternative to batteries for energy storage [1]. In comparison with batteries, supercapacitors have a lower energy density and a higher power density. Supercapacitors can thus be used in a lot of applications for energy storage and management. The main application for supercapacitors is to use them as energy buffers to limit the power constraints on energy sources such as batteries, fuel cells, or decentralised power networks [2], [3]. The use of supercapacitors requires power electronics in order to guarantee an efficient management of such devices. Both the design and the control of their state of charge are sensitive points because they are often connected to several energy sources.

A supercapacitor storage system has been previously studied in simulation for a series hybrid electric vehicle [4]. These studies have revealed several implementation problems. Therefore in this paper, the design and limitations of such a system are studied. Technical requirements and sensitive constraints are also taken into account.

A hybrid electric vehicle can be seen as a multi-source system, where the energy flows coming from each element have to be managed to ensure optimal control. The Energetic Macroscopic Representation (EMR) has been developed to propose a synthetic description of electromechanical conversion systems. A Maximal Control Structure (MCS) can be deduced from EMR using inversion rules [5] in order to propose a more efficient management.

## II. STRUCTURE AND MODELLING OF THE STORAGE SYSTEM

### A. Structure of the storage system

The supercapacitor storage system is used in a series hybrid electric vehicle, which has been previously described in [4] and [6]. As the study is focused on the storage system, two equivalent sources are used. A mono-directional current source represents the generation system composed of the internal combustion engine, the electrical generator and the rectifier. The traction part is simulated using a bi-directional current source in order to allow regenerative braking.

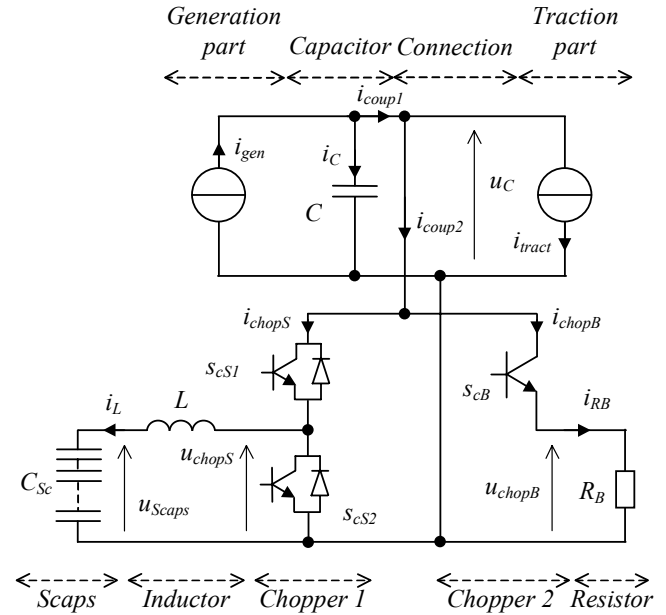


Figure 1. Storage system scheme

The storage system is made of a supercapacitor bank  $C_{sc}$  and a braking resistor  $R_B$  (Fig. 1). A chopper is associated with the supercapacitor bank to interface the difference in voltage level between the storage tank and the main DC bus. The control of this converter make it possible to manage the supercapacitors state of charge.

An inductor  $L$  is added to filter the current in the supercapacitor bank. Another chopper is associated with braking resistors to turn on or off energy dissipation.

On the main DC bus, a capacitor links the various sources and converters.

### B. EMR of the storage system

The Energetic Macroscopic Representation (EMR) is a synthetic graphical tool based on the principle of action and reaction between connected elements [7]. It leads to a synthetic description of an overall conversion system between several sources. In such a representation, coupling devices (overlapped pictograms) distribute energy from upstream or downstream elements (see Appendix). The storage system is described using EMR (top part of Fig. 2) [4].

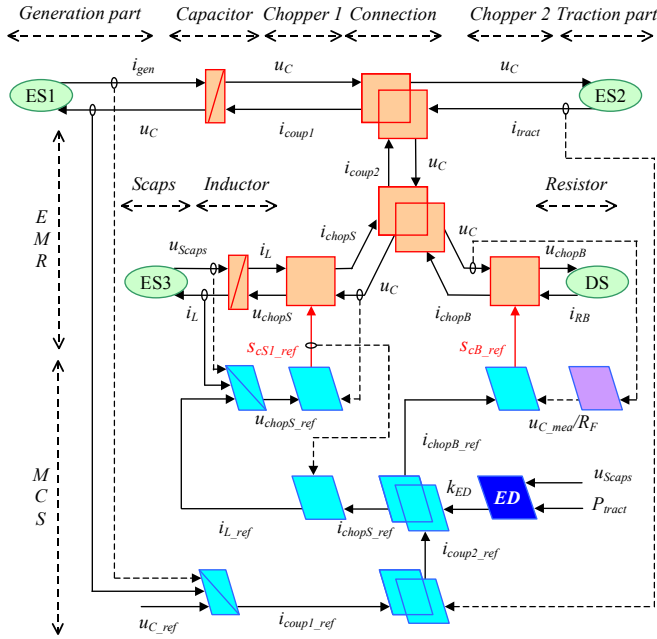


Figure 2. EMR and MCS of the storage system

**Model of the generation part, traction part and supercapacitors** – The generation part is an equivalent electric source, which delivers a charge current  $i_{gen}$ . The traction source generates the current  $i_{tract}$  which can discharge or charge the storage system. These sources are represented by the electric sources (ES1 and ES2) having for input the DC bus voltage  $u_C$ .

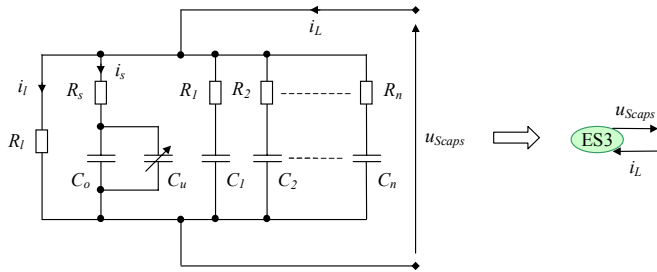


Figure 3. Model of the supercapacitors

The supercapacitor bank is modelled as a voltage source. For the majority of the studied traction applications, the model of Zubieta and Bonert [8] can be used (Fig. 3). This model takes into account a non-linear equivalent capacitance ( $C_o$  and  $C_u$ ), a leakage resistor ( $R_l$ ), a series resistor ( $R_s$ ), and relaxation

phenomenon ( $R_l$ ,  $C_l$ ;  $R_2$ ,  $C_2$ ; ...;  $R_n$ ,  $C_n$ ). Nevertheless, the load and discharge frequencies are weak enough in this application, to neglect relaxation phenomenon. The leakage resistor  $R_l$  is also neglected due to its high value. The supercapacitors are then represented by an electric source (ES3) in Fig. 2 and 3, having for input the filter inductor current  $i_L$  and for output the components voltage  $u_{Scaps}$ .

**Model of the braking resistor** – The braking resistor is activated if the supercapacitors cannot store energy any more. The resistor dissipates the energy excess due to the vehicle deceleration. Its representation can thus correspond to a dissipative source (DS) of energy (copper losses).

**Model of the DC bus capacitor** – A capacitor stores potential energy. It is represented by an accumulation element (orange rectangular pictograms with an oblique bar) whose state variable is the DC bus capacitor voltage. This voltage depends on the current delivered by the generation part  $i_{gen}$  and on the current coming from the traction part and supercapacitors  $i_{coup1}$ :

$$i_C = C \frac{du_C}{dt} = i_{gen} - i_{coup1} \quad (1)$$

where  $C$  is the capacitance.

**Model of the filter inductor** – An inductor stores kinetic energy. It is represented by an accumulation element whose state variable is the filter inductor current  $i_L$ . This current depends on the voltage delivered by the supercapacitors  $u_{Scaps}$  and the output voltage of chopper  $u_{chopS}$ :

$$L \frac{di_L}{dt} + r_L i_L = u_{chopS} - u_{Scaps} \quad (2)$$

where  $L$  is the inductance and  $r_L$  the series resistance of the inductor.

**Model of the electric coupling (parallel connection)** – Electric coupling between the generation part, the supercapacitor bank, the braking resistor and the traction part of the vehicle is represented by overlapped orange square pictograms. This coupling can be divided in two sub-couplings. This enable us to visualise directly the energy flow between the braking resistor and the supercapacitor bank:

$$\begin{cases} i_{coup1} = i_{coup2} + i_{tract} \\ u_{coup1} = u_C \end{cases} \quad (3)$$

$$\begin{cases} i_{coup2} = i_{chopS} + i_{chopB} \\ u_{coup2} = u_C \end{cases} \quad (4)$$

where  $i_{coup1}$ ,  $u_{coup1}$ ,  $i_{coup2}$ ,  $u_{coup2}$  represent the currents and the voltages of the electric coupling 1 and 2,  $i_{tract}$  the traction part current,  $i_{chopS}$  the supercapacitors chopper current and  $i_{chopB}$  the braking chopper current.

**Model of the choppers** – Choppers are electric converters (without energy accumulation) represented by orange square pictograms. The choppers are described by the following relationships:

$$\begin{cases} u_{chopS} = s_{cSI} u_C \\ i_{chopS} = s_{cSI} i_L \end{cases} \text{ with } s_{cSI} \in \{0;1\} \quad (5)$$

$$\begin{cases} u_{chopB} = s_{cB} u_C \\ i_{chopB} = s_{cB} i_{RB} \end{cases} \text{ with } s_{cB} \in \{0;1\} \quad (6)$$

with  $s$  the switching functions,  $u_C$  the capacitor voltage,  $i_L$  the inductor current and  $i_{RB}$  the braking resistor current.

When averaged value modelling is used, the switching functions are replaced by duty cycles (in this case the braking chopper current  $i_{chopB}$  equals the braking resistor current  $i_{RB}$ ):

$$\begin{cases} u_{chopS} = \alpha_{chopS} u_C \\ i_{chopS} = \alpha_{chopS} i_L \end{cases} \text{ with } \alpha_{chopS} \in [0;1] \quad (7)$$

$$\begin{cases} u_{chopB} = \alpha_{chopB} u_C \\ i_{chopB} = i_{RB} \end{cases} \text{ with } \alpha_{chopB} \in [0;1] \quad (8)$$

where  $\alpha$  are the duty cycles.

### C. Influence of filter resistance

For low values of the duty cycle  $\alpha_{chopS}$ , the ratio  $U_C/U_{Scaps}$  differs from  $1/\alpha_{chopS}$  when the resistance  $r_L$  of the filter inductor is taken into account (for this study the capacitor voltage, traction and generation current are considered without ripple in steady state:  $u_C = U_C$ ,  $i_{tract} = I_{tract}$ ,  $i_{gen} = I_{gen}$ ) [9], [10]:

$$U_C = U_{Scaps} \frac{\alpha_{chopS}}{\alpha_{chopS}^2 + \frac{r_L}{R}} \text{ with } R = \frac{U_C}{I} = \frac{U_C}{I_{tract} - I_{gen}} \quad (9)$$

The voltage across the load increases when the duty cycle  $\alpha_{chopS}$  decreases (or when  $(1-\alpha_{chopS})$  increases). It reaches its maximal value  $U_{C\_max}$  for  $\alpha_{chopS\_min}$ :

$$U_{C\_max} = \frac{U_{Scaps}}{2 \alpha_{chopS\_min}} \text{ where } \alpha_{chopS\_min} = \sqrt{\frac{r_L}{R}} \quad (10)$$

Thereafter, the voltage decreases and tends towards zero as  $\alpha_{chopS}$  tends towards zero. The ratio between  $U_C$  and  $U_{Scaps}$  for several values of  $r_L$  is represented in Fig. 4.

To reach high values of  $U_C/U_{Scaps}$ , it is thus necessary to have  $r_L$  much lower than  $R$ . On the other hand,  $U_C/U_{Scaps}$  increases when  $\alpha_{chopS}$  decreases ( $(1-\alpha_{chopS})$  increases). The supercapacitors current must then be greater than:

$$I_{L\_max} = -\frac{U_{Scaps}}{2 r_L} \quad (11)$$

A linear control can only be used for monotonous systems, i.e. the systems for which the output evolves in the same direction as the input. If the parameters are well tuned, the loop caused by the control leads to stable feedback. For non-monotonous systems, the feedback generated can lead to instability.

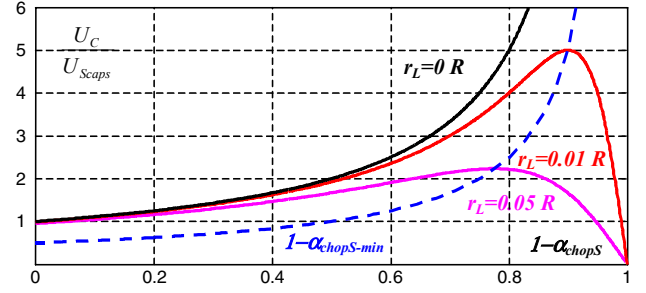


Figure 4. Voltage ratio vs. duty cycle  $\alpha_{chopS}$

The maximum voltage ratio depends on the traction current required by the vehicle. Due to this phenomenon the system can become unstable. The inductance design must take into account this problem to avoid instability. For a given value of  $L$  and  $r_L$ , the duty cycle  $\alpha_{chopS}$  must be higher than a limit value, as shown in Fig. 4.

Note that for these calculations, on-resistors of the diodes and transistors can be added. But as they remain weak in comparison with the inductance series resistor, they are neglected.

## III. MAXIMUM CONTROL STRUCTURE OF THE STORAGE SYSTEM

From the EMR of a system, one can deduce a Maximum Control Structure (MCS) using inversion rules. The MCS is elaborated using the maximum number of control operations and measurements. Controllers are depicted by parallelograms with an oblique bar (see Appendix). The MCS of the storage system has already been proposed in [4] (bottom part of Fig. 2).

### A. Control of the supercapacitor bank

In order to manage the system, the DC bus voltage  $u_C$  must have a constant value. Moreover the current delivered by the inductor has to be maintained within given limits to ensure a high efficiency. The principal difficulty is that the supercapacitor chopper is a two quadrant DC/DC converter. There is then only one degree of freedom (switching function of the chopper) to control the DC bus voltage and to control the current in the supercapacitors. A tuning chain connects the switching function  $s_{cSI}$  of the supercapacitor chopper to the DC bus voltage  $u_C$ .

The inversion of this chain requires two controllers (DC bus voltage and inductor current) to manage the energy stored in the supercapacitor. From these requirements, the chopper control is identified by direct inversion of EMR (see Fig. 2).

The DC bus voltage has to be maintained at a constant value in spite the variable dynamics of currents  $i_{gen}$  and  $i_{tract}$ . A voltage controller and current compensations are thus used.

The inductor current controller of the inner loop has thus to have a faster response time. As the current is disturbed by the supercapacitor voltage, a voltage compensation is also made [11], [12].

### B. Control of the braking resistor

When the braking resistor system is active, the supercapacitors are disabled. The DC bus voltage control is not carried out any more by the supercapacitor chopper. Thus the braking chopper must regulated the DC voltage. The objective is to maintain the value of  $u_C$  by acting on the switching function of the braking chopper  $s_{cB}$ . The MCS is deduced from Fig. 2. The tuning chain connects the switching function  $s_{cB}$  of the braking chopper to the DC bus voltage  $u_C$ . The inversion of this chain forces the energy to dissipate during regenerative operation when the supercapacitor voltage reaches its maximum value.

To control the braking resistance chopper, it is necessary to measure the current through it. Nevertheless as this current is switched via the voltage  $u_{chopB}$  one cannot measure it. An estimation block (purple parallelogram pictograms) is then set up. This block governs the following equations:

$$\alpha_{chopB} = \frac{u_{chopB}}{u_C} = \frac{R_B i_{RB}}{u_C} = \frac{i_{chopB}}{\frac{u_C}{R_B}} \quad (12)$$

where  $\alpha_{chopB}$  is the duty cycle of the braking chopper.

### C. Global control

Both tuning chains are linked with a coupling device (parallel connection). In the EMR methodology, a distribution criterion is required in the control scheme to define each reference. A strategy block has been added to define the energy distribution criterion  $k_{ED}$  (see Fig. 2) between the supercapacitors and the braking resistor:

$$\begin{cases} i_{chopB\_ref} = k_{ED} i_{coup2\_ref} \\ i_{chopS\_ref} = (1 - k_{ED}) i_{coup2\_ref} \end{cases} \quad (13)$$

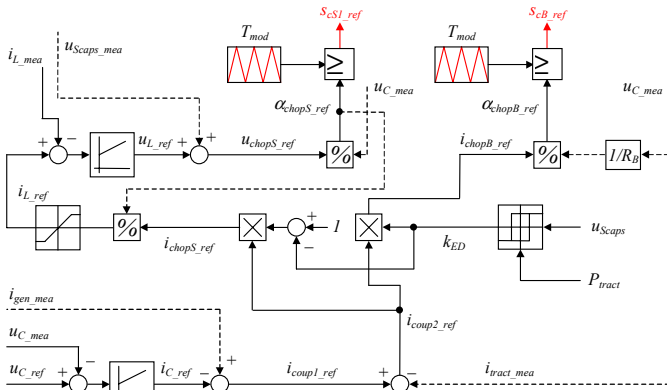


Figure 5. Bloc diagrams of the supercapacitor bank and braking resistor control

By acting on  $k_{ED}$ , we can activate both subsystems:

- if the traction power  $P_{tract}$  is negative and the voltage  $u_{Scaps}$  is maximum, then the dissipation chopper is activated ( $k_{ED} = 1$ ),

- if the voltage  $u_{Scaps}$  is lower then its maximal value, the supercapacitor chopper is activated for any traction power ( $k_{ED} = 0$ ).

It enables a supercapacitor to charge or discharge according to the traction requirements. Moreover it activates the braking resistor as a function of the supercapacitor maximum voltage.

In order to familiarise the reader with EMR and MCS, a detailed representation of the control supercapacitors chopper and braking resistor is shown by using bloc diagrams (Fig. 5).

## IV. EXPERIMENTAL RESULTS

### A. Stability of the system

The aim of the first experimentation is to check the instability of the system for low values of the duty cycle  $\alpha_{chopS}$  as a function of the internal inductor resistor. The results of this experiment will be compared to those obtained by simulation.

As the instability of the system occurs for low values of the duty cycle  $\alpha_{chopS}$ , the study will be done for a discharge of the supercapacitors. This will be carried out using a resistor  $R_d$  and a power converter in order to control the current at the output of the discharge chopper  $i_{chopd}$  (Fig. 6). The conditions for this test are as follows:

$$\begin{aligned} C &= 2200 \mu F & L &= 74 \text{ mH} \\ r_L &= 205 \text{ m}\Omega & R_d &= 22,7 \Omega \\ C_{Sc} &= 4.83 \text{ F} & u_{Scaps}(t=0 \text{ s}) &= 70 \text{ V} \\ u_{C\_ref} &= 250 \text{ V} & \text{Switching frequency } f &= 2 \text{ kHz} \end{aligned}$$

The supercapacitor bank used corresponds to 12 Maxwell BOOSTCAP Ultracapacitor BPAK0350-15EA of 58 F / 15 V in series.

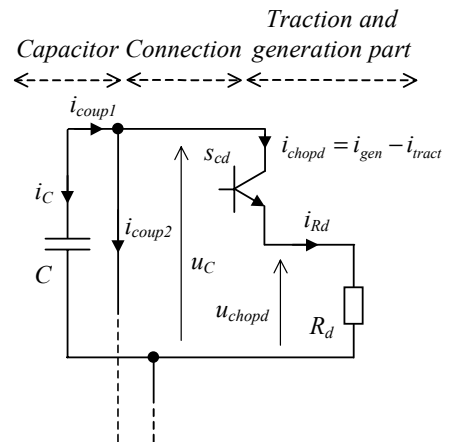


Figure 6. Storage system scheme for instability study

A comparison between experimentation via a dSPACE controller board (Fig. 7) and simulation in averaged value via Matlab-Simulink™ is provided. It should be noticed that the experimentation involves current ripple unlike in the simulation.



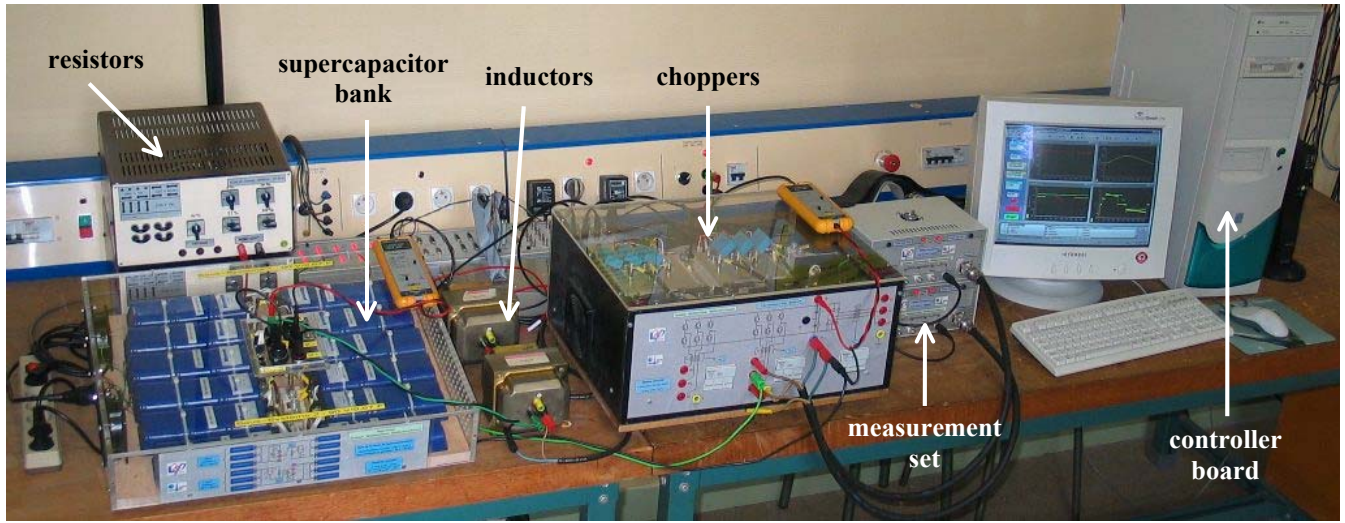


Figure 7. Experimental Set-up

Fig. 8 and 9 show the experimental and simulation results of the input voltage  $u_{Scaps}$  and the output voltage  $u_C$  versus time  $t$  of the buck-boost converter. From  $t=0$  s, no-load is necessary, the DC bus controller regulates the DC bus voltage  $u_C$  to the desired reference value, i.e. 250 V (Fig. 8). The initial voltage of the supercapacitors  $u_{Scaps}$  is regulated at 70 V (Fig. 9).

At  $t=5$  s, a current step  $i_{chopd}$  of 1 A is imposed. This leads to the discharge of the supercapacitor. The chopper is in boost operation and the DC bus voltage is fixed a constant value. As the supercapacitors current increases the discharge becomes stronger. When the relationship (10) is valid, i.e. at  $\alpha_{chops}$  equals  $\alpha_{chops-min}$ , the ratio  $U_C/U_{Scaps}$  cannot increase any more (see Fig. 4). Consequently the DC bus voltage can no longer be controlled. The system becomes unstable and the DC bus voltage  $u_C$  falls brutally (Fig. 8). In order to avoid excessive currents in the supercapacitors, the reference current of the filter inductor is limited (see Fig. 5). When the system becomes unstable, the current falls abruptly. It is then saturated at 25 A (Fig. 10).

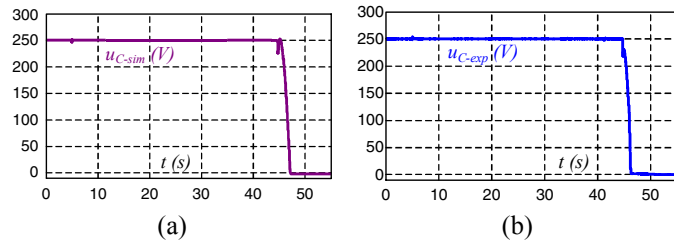


Figure 8. DC bus voltage for  $i_{chopd} = 1$  A  
(a) simulation (b) experimentation

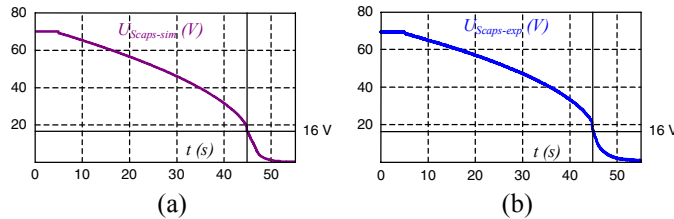


Figure 9. Supercapacitor bank voltage for  $i_{chopd} = 1$  A  
(a) simulation (b) experimentation

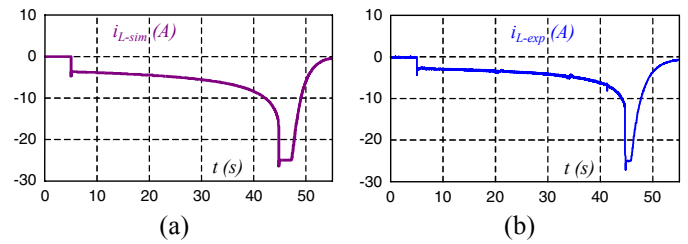


Figure 10. Supercapacitor bank current for  $i_{chopd} = 1$  A  
(a) simulation (b) experimentation

As described in (10), the increase of current  $I$  leads to a decrease of ratio  $U_{C-max}/U_{Scaps}$ . Thus, for high value of current, instability occurs quicker than for low values. In Fig. 11, 12 and 13, the same test is carried out for a step current  $i_{chopd}$  of 2 A. Consequently, instability occurs at a voltage of the supercapacitor higher than for the first test (approximately 26 V in comparison with 16 V).

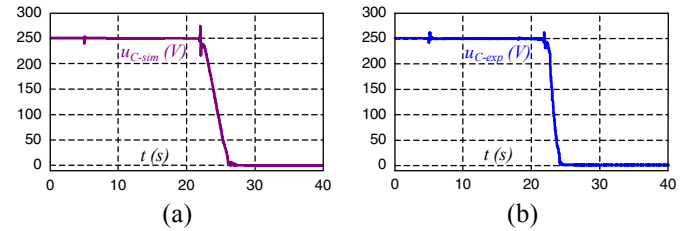


Figure 11. DC bus voltage for  $i_{chopd} = 2$  A  
(a) simulation (b) experimentation

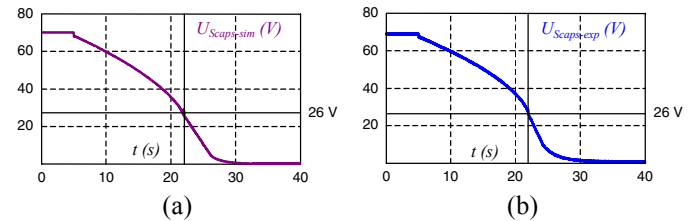


Figure 12. Supercapacitor bank voltage for  $i_{chopd} = 2$  A  
(a) simulation (b) experimentation

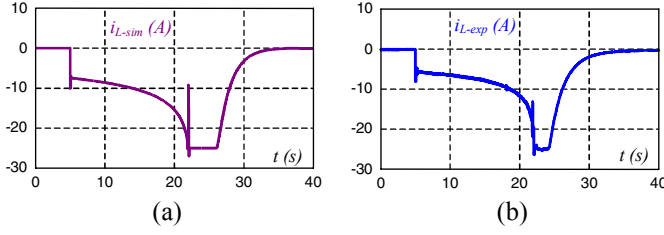


Figure 13. Supercapacitor bank current for  $i_{chopd} = 2 A$   
(a) simulation (b) experimentation

The differences between experimentation and simulation are due to the use of average values in the simulation, the fact that resistors of the diodes and transistors are neglected in the simulation and the use of sampling and quantization in the experimentation.

Instabilities occur earlier when the loading current is high. This operating mode must thus be avoided. Moreover, the efficiency is reduced in this operating range :

- A supercapacitor contains an internal series resistor. If this is passed through by a high current, the losses which results will be all the more important. This decreases the supercapacitors efficiency. The energy efficiency of the discharge with a constant current can be expressed using the following relationship found in [13]:

$$\eta_{Scaps} = 1 - 2 R_S \frac{i_L}{U_{Scap-max}} \frac{100}{100 + d} \quad (14)$$

with  $R_S$  the supercapacitor series resistor,  $U_{Scap-max}$  the supercapacitor maximum voltage,  $i_L$  the supercapacitor current and  $d$  the voltage discharge ratio expressed as a percentage of the difference between the maximum voltage  $U_{Scap-max}$  and the final voltage  $U_{Scap-fin}$  ( $d = 100 U_{Scap-fin}/U_{Scap-max}$ ).

- The buck-boost converter efficiency varies according to the required current. It is described by the following relationship [14]:

$$\eta_{chopS} = \frac{I}{I + \frac{r_L}{\alpha_{chopS}^2 R}} \text{ with } R = \frac{U_C}{I} = \frac{U_C}{I_{tract} - I_{gen}} \quad (15)$$

In Fig. 14 and 15 the efficiency of the supercapacitors and the buck-boost converter are represented. One can verify that the current  $i_{chopd}$  is higher and the efficiency is reduced.

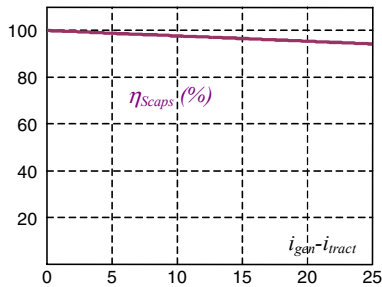


Figure 14. Efficiency of bank supercapacitor  $12*58 F / 0.019 m\Omega$   
for  $d=10 \%$  and  $U_{Scap-max}=15 V$

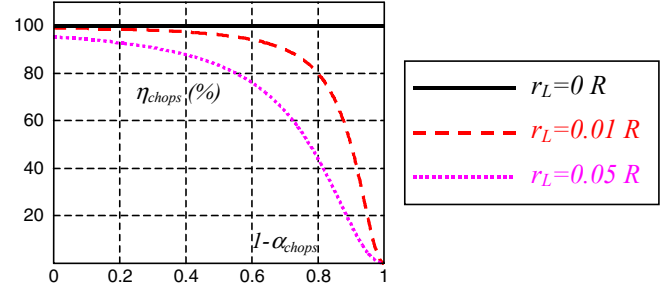


Figure 15. Efficiency of buck-boost converter

It should be noticed that new converter structures are created in order to allow a greater duty cycle without deteriorating the energetic efficiency [14].

### B. Normal operating

In order to check the correct operation for the control, a test cycle was carried out. The conditions for this experimentation are as follows:

$$\begin{aligned} C &= 2200 \mu F & L &= 174 mH \\ L_2 &= 172 mH & R_B &= 46 \Omega \\ R_2 &= 49,3 \Omega & V_{DC} &= 150 V \\ C_{Sc} &= 4.83 F & u_{Scaps}(t=0 s) &= 100 V \\ u_{Scaps-max} &= 150 V & u_{C ref} &= 250 V \\ \text{Switching frequency } f &= 3 \text{ kHz} \end{aligned}$$

The supercapacitors tank is as described in the previous section. To test the system easily the structure studied is presented in Fig. 16.

The traction and generation parts are represented by a DC current source through  $V_{DC}$  and  $L_2$  for the load mode and of a resistor  $R_2$  for the discharge mode. For a traction operating cycle the supercapacitors energy is discharged in the resistor  $R_2$ . In braking or generation operating cycle the energy coming from the DC current source ( $V_{DC}$  and  $L_2$ ) charges the supercapacitors or is dissipated in the braking resistor.

For the current profile of the DC current source (Fig. 17), the terminal voltage of the supercapacitors varies between its maximum value (adjusted to  $150 V$ ) and  $2/3$  of the maximum value ( $100 V$ ) (Fig. 19).

When the supercapacitors voltage  $u_{Scaps}$  reaches its maximum value ( $t_3$ ), the load stop of the double layer capacitor is obtained from the energy distribution criterion  $k_{ED}$  ( $k_{ED} = 1$  in Fig. 2 and 5) causing the cancellation of the supercapacitors current  $i_L$  (Fig. 18). From this moment the braking chopper is switched on and the braking energy via the DC current source is dissipated in the braking resistors (Fig. 20).

When the traction power becomes negative, the supercapacitors are activated ( $k_{ED} = 0$ ) and the braking resistor is disconnected ( $t_5$ ). The DC bus voltage  $u_C$  is well controlled (Fig. 21). The displayable jump of voltage on the Fig. 19 ( $t_3$ ) is due to supercapacitor series resistor.

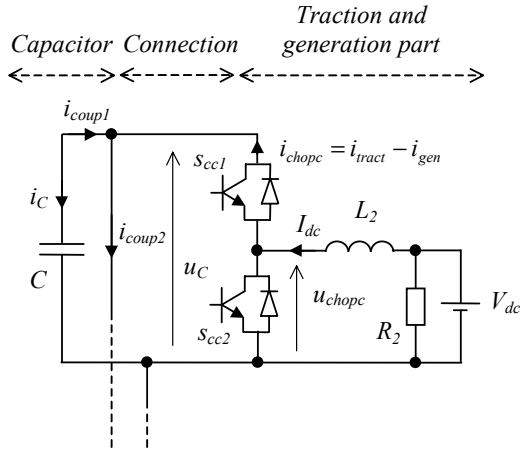


Figure 16. Storage system scheme for normal operating study

## V. CONCLUSION

A supercapacitor storage system has been designed for a traction application. The Maximum Control Structure (MCS) of the system has been deduced from the Energetic Macroscopic Representation (EMR) description using an inversion methodology. Experimentation results show the ability of the system to store energy during the braking operation with a limitation on the supercapacitor voltage by acting on the braking resistor. Close attention has been paid to the instability of the system due to the inductor resistor.

## REFERENCES

- [1] A. Schneuwly, R. Gallay, "Properties and applications of supercapacitors, from the state-of-the-art to future trends", *PCIM'2000*, Nuremberg (Germany), 2000.
- [2] A. Rufer, P. Barrade, "A Supercapacitor-Based Energy Storage System for Elevators with Soft Commutated Interface", *IEEE-IAS'2001*, Chicago, October 2001, vol. 2, pp. 1413 -1418.
- [3] R. Kötzt, S. Müller, M. Bärtschi, B. Schnyder, P. Dietrich, F. N. Büchi, A. Tsukada, G. G. Scherer, P. Rodatz, O. Garcia, P. Barrade, V. Hermann, R. Gallay, "Supercapacitors for peak-power demand in fuel-cell-driven cars", *Electro-Chemical Society annual meeting*, San Francisco, September 2001.
- [4] W. Lhomme, Ph. Delarue, P. Barrade, A. Bouscayrol, "Maximum Control Structure of a series Hybrid Electric Vehicle using supercapacitors", *EVS'21*, Monaco, April 2005.
- [5] A. Bouscayrol, Ph. Delarue, "Simplifications of the Maximum Control Structure of a wind energy conversion system with an induction generator", *International Journal of Renewable Energy Engineering (IJREE)*, August 2002, vol. 4, no. 2, pp. 479-485.
- [6] W. Lhomme, A. Bouscayrol, P. Barrade, "Simulation of series hybrid electric vehicles based on Energetic Macroscopic Representation", *IEEE-ISIE '04*, Ajaccio, May 2004, pp. 1525-1530.
- [7] A. Bouscayrol, Ph. Delarue, "Weighted control of drives with series connected DC machines", *IEEE-IEMDC'03*, Madison (USA), June 2003, pp. 159-165.
- [8] L. Zubieta, R. Bonert, "Characterization of double-layer capacitors for power electronics applications", *IEEE Transactions on Industry Applications*, January-February 2000, vol. 36, issue. 1, pp. 199-205.
- [9] K. Harada, E. Sakai, F. Anan, K. Yamasaki, "Basic characteristics of electric double-layer capacitors controlled by switching converters", *INTELEC '96*, 18th International, 6-10 Oct. 1996, pp. 491 - 498.
- [10] R. Bausière, F. Labrique, G. Segui, "Les convertisseurs de l'électronique de puissance, vol. 3 : La conversion continu - continu", 2<sup>nd</sup> Edn. (Technique & Documentation, 1997), pp. 131-137.

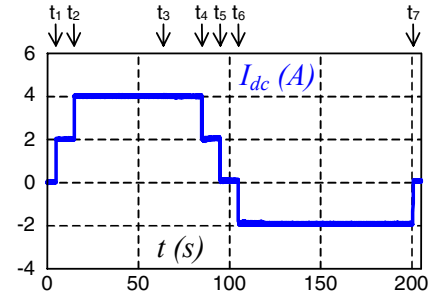


Figure 17. Current of the DC current source

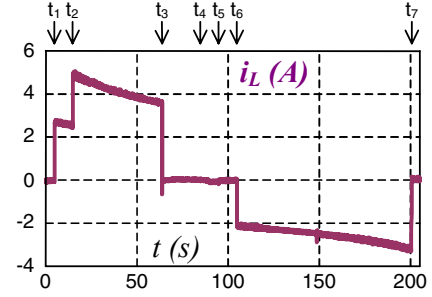


Figure 18. Current of the supercapacitor bank

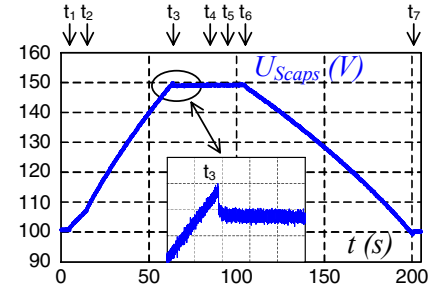


Figure 19. Voltage of the supercapacitor bank

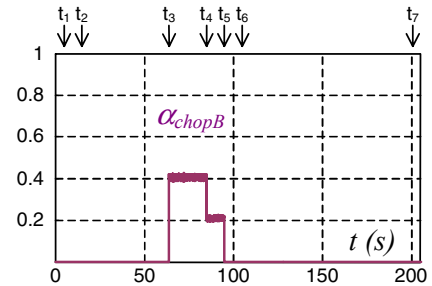


Figure 20. Averaged duty cycle of the braking chopper

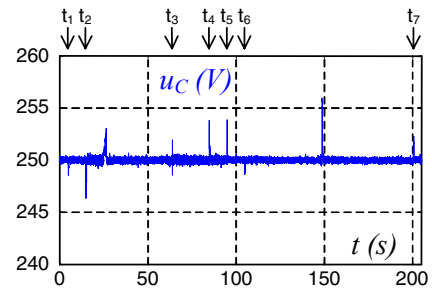


Figure 21. Voltage of the DC bus



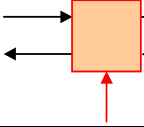
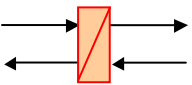
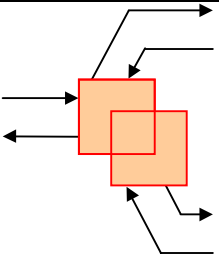
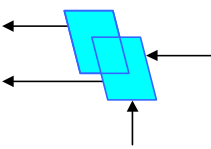
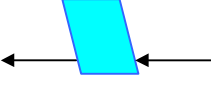
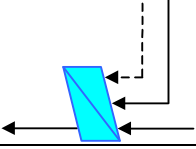
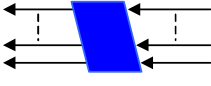
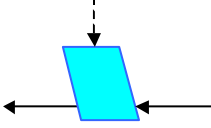
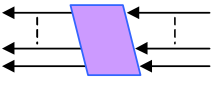
[11] B. J. Arnet, L. P. Haines, "High Power DC-to-DC Converter for Supercapacitors", *IEEE-IEMDC 2001*, Cambridge, June 2001, pp. 985-990.

[12] M. Ortuzar, J. Dixon, J. Moreno, "Design, construction and performance of a buck-boost converter for an ultracapacitor-based auxiliary energy system for electric vehicles", *IECON '03, The 29th Annual Conference of the IEEE*, vol. 3, 2-6 Nov. 2003, pp. 2889 - 2894.

[13] P. Barrade, A. Rufer, "Current capability and power density of supercapacitors: considerations on energy efficiency", *EPE 2003: European Conference on Power Electronics and Applications*, 2-4 September, Toulouse, France.

[14] K. C. Tseng, T. J. Liang, "Novel high-efficiency step-up converter", *IEEE-Electric Power Applications*, vol. 151, no. 2, 9 March 2004, pp. 182 - 190.

APPENDIX: SYNOPTIC OF ENERGETIC MACROSCOPIC REPRESENTATION

	Electrical source of energy		Dissipative source of energy (copper losses)		Electrical converter (without energy accumulation)
	Element with energy accumulation		Electrical coupling (distribution of electric energy)		Control block with coupling criterion
	Control block without measure and controller		Control block with controller		Strategy block
	Control block with measure without controller		Estimation block	-----	Disturbance rejection (optional)
				0	Sensor